Electronic Supplementary Material (ESI) for Journal of Materials Chemistry A
This journal is © The Royal Society of Chemistry 2014

Supporting Information

Sulfur-infiltrated three-dimensional graphene-like material with hierarchical pores for highly stable lithium-sulfur batteries

Yunyong Li, Zesheng Li,Qinwei Zhang and Pei Kang Shen*

State Key Laboratory of Optoelectronic Materials and Technologies, and Key Laboratory of Low-Carbon Chemistry & Energy Conservation of Guangdong Province, School of Physics and Engineering, Sun Yat-sen University, Guangzhou, 510275 (PR China) E-mail: stsspk@mail.sysu.edu.cn

Experimental

Synthesis of 3D GlM. The 3D GlM was synthesized by an improved method as previously reporte[S1]. Typically, the pretreated macroporous acrylic type cation exchange resin (10 g, Shanghai Hualing Resin Co., Ltd, China) was impregnated with targeting ions of nickel in 0.10 mol L^{-1} nickel acetate (Shanghai Hebao Chemical Co., Ltd. China) solution (100 mL) for 6 h. The exchanged resin was washed with deionized water and dried at 60 ^{o}C for 12 h. Then, the exchanged resin (10 g) was added into a 400 mL KOH/ethanol solution containing 50 g KOH and stirred at 80 ^{o}C until the mixture solution became an 'ink-paste', followed by another 6 h of static soaking in ambient conditions. After that, the mixture solution was dried at 70 ^{o}C for 48 h and then smashed by a disintegrator. Finally, the mixture was heated at 850 ^{o}C for 2 h in N_2 atmosphere with a heating rate of 2 ^{o}C min^{-1} and an N_2 flow rate of 60 cc min^{-1}. After cooling down to room temperature, the resulting sample was added into 3 mol L^{-1} HCl solutions with a specific volume for more than 12 h at magnetic stirring. Afterwards, the sample was repeatedly washed by de-ionized water until a pH value of 7 was reached and dried at 70 ^{o}C in ambient for 12 h.

Synthesis of 3D GlM/S nanocomposites and 3D GlM+69.7 wt%S. At first, the pretreatment of 3D GlM sample was conducted at 200 ^{o}C under vacuum condition for 10 h to remove water and other impurities which adsorb in the surface of 3D GlM. Secondly, the pretreated 3D GlM and elemental sulfur with various weight ratios (1:0.8, 1:2, and 1:3) were mixed together and placed in a sealable glass tube and then sealed (Fig. S9, A), respectively. After that, the mixture was heated to 155 ^{o}C for 10 h with a heating rate of 1 ^{o}C min^{-1} in a near-vacuum (Fig. S9, B), respectively. For comparison, the 3D GlM+69.7 wt%S sample with the weight ratios (3:7) of the pretreated 3D GlM and elemental sulfur, was also made by the same process but without melt-diffusion process.

Characterization. The X-ray diffraction (XRD) measurements were carried out in a D/Max-III (Rigaku Co., Japan) using CuK α radiation with a scanning rate of 10^{o} min^{-1}, operating at 40 kV and 30 mA. The samples were grinded with an agate mortar until they could pass a 325 mesh standard sieve. The transmission electron microscopic (TEM) investigations were carried out in a FEI Tecnai G2 F30 at 300 kV. Scanning electron microscopy (SEM) micrograms were collected on a JEM-6700F field emission scanning electron microscope. X-ray photoelectron spectroscopy (XPS) was conducted with two separate systems equipped with monochromatic Al K sources (ESCALab250, USA) to analyze the chemical composition of the samples. The N_2 adsorption experiments using an ASAP-2420 Surface Area Analyzer (Micrometeritics Co., USA) were conducted to investigate the porosity of the samples. The 3D GlM and 3D GlM/S nanocomposities were outgassed at 200 ^{o}C and room temperature in a nitrogen flow for 4 h with an evacuation rate of 2 mmHg s^{-1} prior to the measurement, respectively. Nitrogen adsorption data were recorded at the liquid nitrogen temperature (77 K). The specific surface area of all the samples was calculated according to the Brunauer-Emmett-Teller (BET) equation from the adsorption data in the relative pressure from 0.05 to 0.2. The total pore volumes were estimated to be the liquid volume of adsorption (N_2) data relative pressure of 0.98. The pore size distribution was determined by the density functional theory (DFT) method. Thermo-gravimetric analysis (TGA) was conducted on a thermo-gravimetry-differential scanning calorimetry instrument (NETZSCHSTA 409 PC) under nitrogen protection at a heating rate of 10 ^{o}C min^{-1} from 30 to 800 ^{o}C.

Electrode fabrication and electrochemical measurements. The cathode slurry were prepared by mixing 80 wt% 3D GlM/S nanocomposites or 3D GlM+69.7 wt%S sample, 10 wt% acetylene black, and 10 wt% polyvinylidene difluoride (PVDF) in N-Methylprrolidone (NMP) solvent dispersant, respectively. Positive electrodes were produced by coating the slurry on aluminum foil to form ~100 μm film and drying in vacuum oven at 60 °C for 24 h. After that, the dried material was pressed and then cut into 1.54 cm^2 (Diameter = 1.4 cm) disk. Preliminary cell tests were done with a 2032 coin-type cells, which were fabricated in an argon-filled glove box using lithium metal as the counter electrode and a microporous polyethylene separator. The electrolyte solution was 1 mol L^{-1} bis-(trifluoromethane)sulfonimide lithium (LiTFSI) in a mixed solvent of dimethoxyethane (DME) and dioxolane (DOL) with a volume ratio of 1:1. This electrolyte was chosen to optimize high-rate behavior because of its lower viscosity and high ionic conductivity. The charge-discharge performance of the cells was tested a program-controlled test system (Shenzhen Neware Battery Co., China), and potential window was controlled between 1.5 and 3.0 V at room temperature. The cyclic voltammetry (CV) and electrochemical impedance spectroscopy measurements (Potential: 3 V, Amplitude: 5 mV, Frequency: 10 mHz~100 kHz) were recorded by a Bio-logic VMP3 electrochemical work station (France). The energy density was calculated on the mass of elemental sulfur.

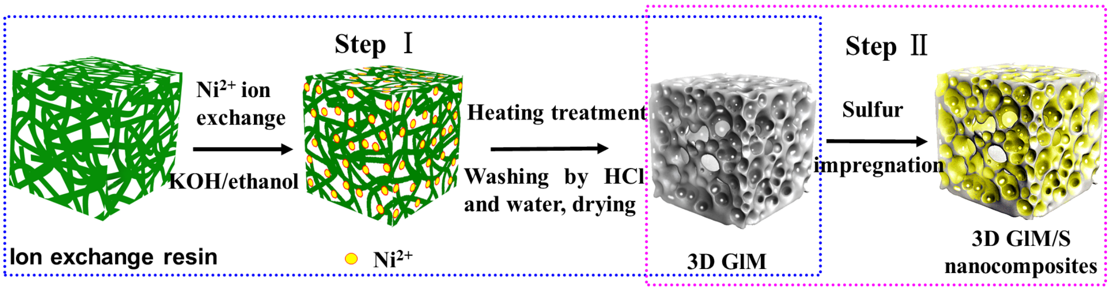

Fig. S1. The synthesis steps of 3D GlM (Step I) and 3D GlM/S nanocomposities (Step II).

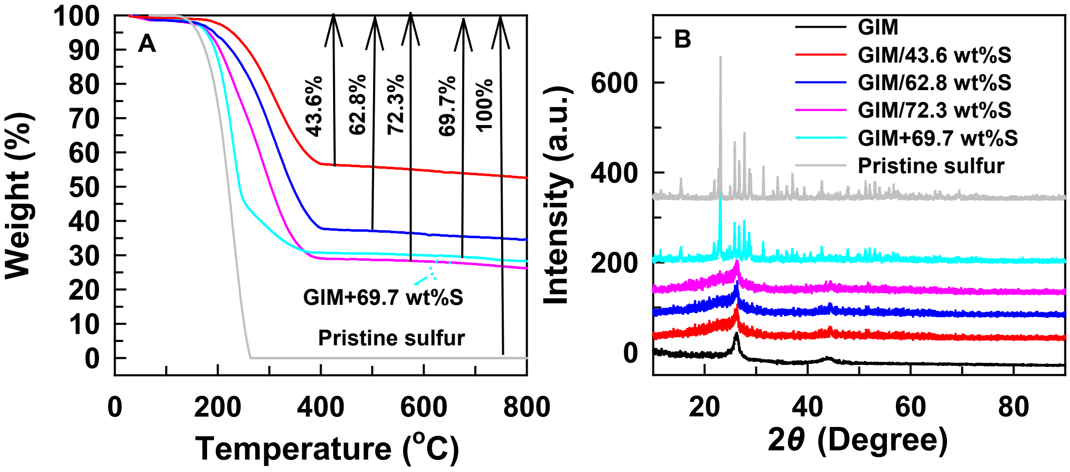

Fig. S2. (A) Thermo-gravimetric analysis (TGA) results of the 3D GlM/S samples, 3D GlM+69.7 wt %S sample and pristine sulfur (The TGA was conducted under nitrogen protection at a heating rate of 10 °C min^{-1} from 30 to 800 °C), (B) XRD profiles of 3D GlM, 3D GlM/S composites with different sulfur contents, 3D GlM+69.7 wt %S sample and pristine sulfur.

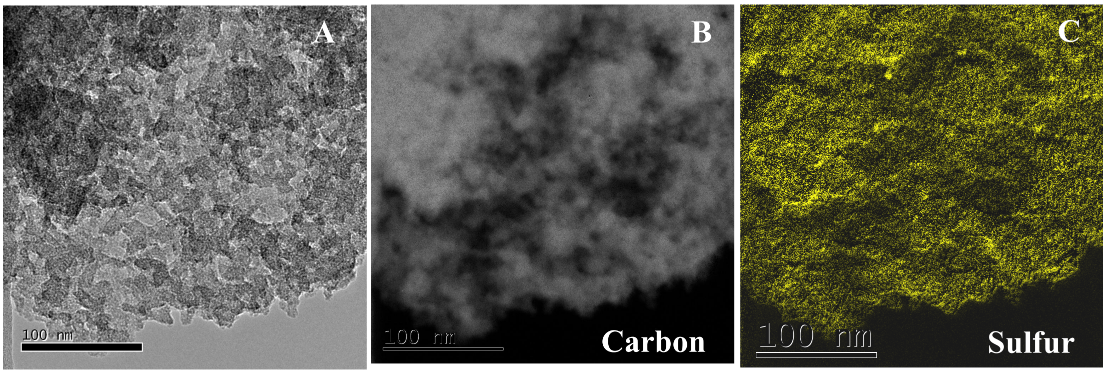

Fig. S3. TEM image (A) of mesoporous graphene-like wall and the corresponding elemental mapping of carbon (B) and sulfur (C), which demonstrates the homogeneous distribution of sulfur.

Compared with the sample of HOPG, a similar sharp peak of C=C for 3D GlM are observed, indicating a good structure of graphitization for 3D GlM (Fig. S4).

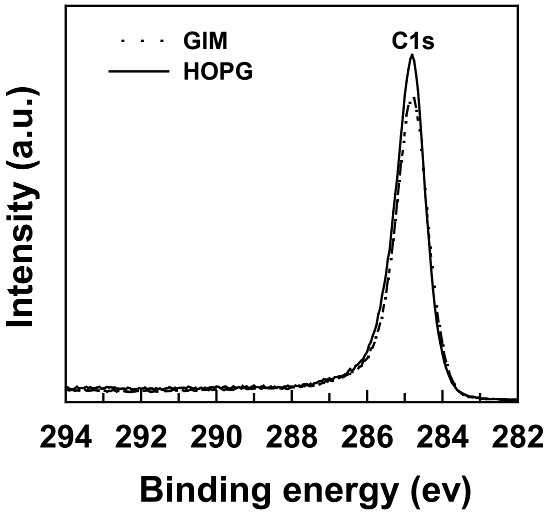

Fig. S4. XPS C1s spectra of 3D GlM and highly oriented pyrolytic graphite (HOPG).

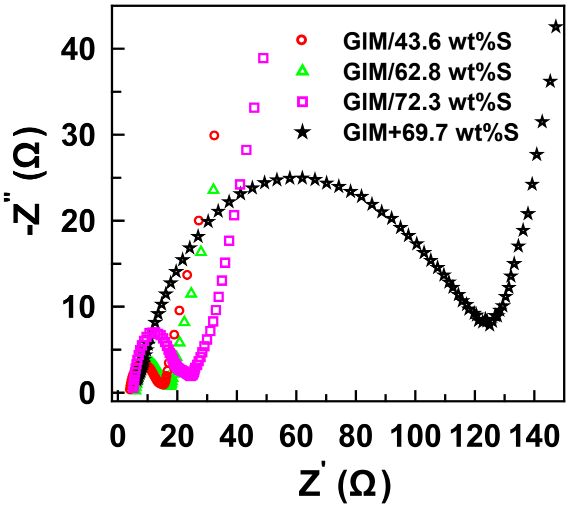

Fig. S5. Electrochemical impedance spectrum of various cathode materials after 100 cycles.

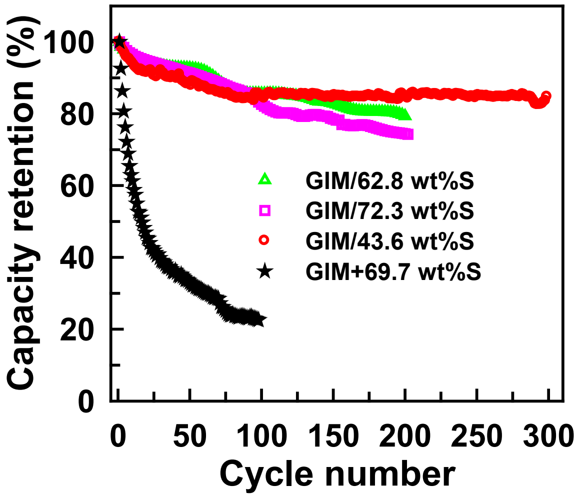

Fig. S6. Cyclic stability of various cathode materials at a discharge rate of 0.5 C.

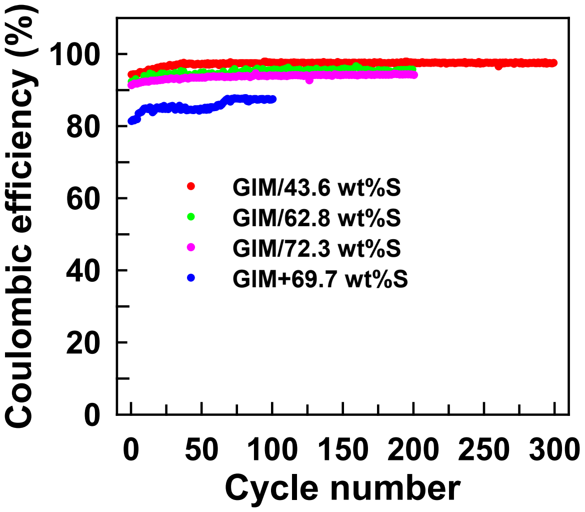

Fig. S7. Coulombic efficiencies of various cathode materials under at a rate of 0.5 C.

The 3D GlM/S nanocomposites (42.6 and 72.3 wt%S) exhibit initial discharge capacity of 1292 mAh g^{-1} and 1195 mAh g^{-1} at 0.2 C, and remain 876 mAh g^{-1} (~68% capacity retention) and 720 mAh g^{-1} (~60% capacity retention) at 3C, respectively (Fig. S8). Moreover, when the discharge rate goes back to 0.5 C, the discharge capacity can be recovered to 1167 mAh g^{-1} and 1020 mAh g^{-1}, respectively.

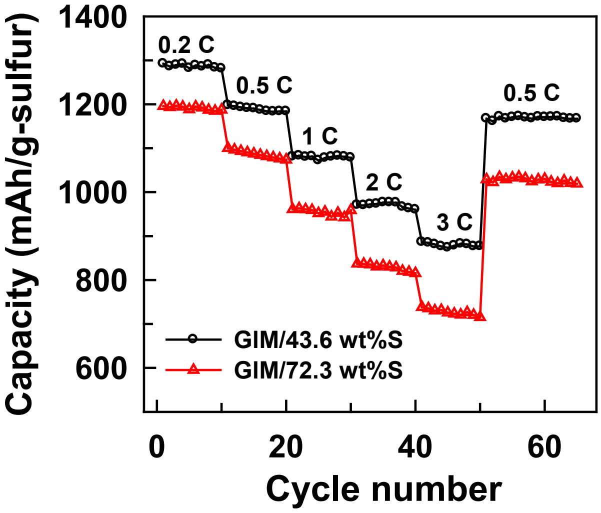

Fig. S8. Discharge specific capacity versus current densities for the 3D GlM/S nanocomposite electrodes.

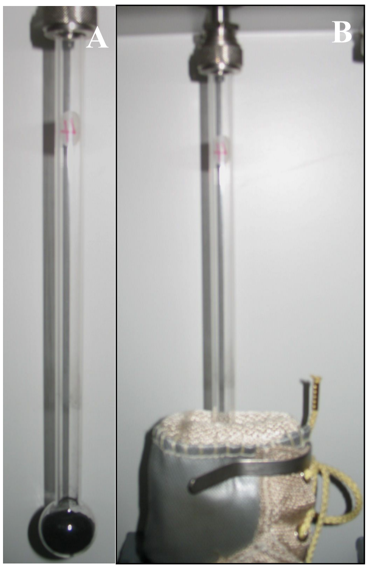

Fig. S9. (A) Sealable glass tube and (B) the further heating device.

Table S1. Physical characteristics of 3D GlM and 3D GlM/S nanocomposites.

Samples Parameters	3D GlM	3D GlM/43.6 wt %S	3D GlM/62.8 wt %S	3D GlM/72.3 wt %S
Mass ratio of 3D GlM and sulfur		1:0.8	1:2	1:3
BET total surface area (m^2 g^{-1})	2700	1220	568	85
Total pore volume (cm^3 g^{-1})	2.50	1.31	0.91	0.45
Microporous volume[a] (cm^3 g^{-1})	1.09	0.47	0.22	0.04
Mesoporous volume (2~7 nm)[b] (cm^3 g^{-1})	0.97	0.30	0.16	0.02
Large pore volume (> 7 nm) (cm^3 g^{-1})	0.44	0.54	0.53	0.39
Conductivity (S m^{-1})	1224	1205	1111	1005

[a]The pore volumes were estimated to be the liquid volume of adsorption (N_2) data relative pressure of 0.16; [b]The difference value between the pore volume (<7 nm) estimated to be the liquid volume of adsorption (N_2) data at relative pressure of 0.70 and the microporous volume.

Table S2. Comparison of the performances of the Li-S batteries based on the 3D GlM/S nanocomposites with those of other typically graphene-sulfur composite materials.

Classification	BET (m^2 g^{-1})	S content (wt%)	Cycle performance (1 C =1675 mA g^{-1})	Ref.
PEG modified GO-carbon black		70	520 mAh g^{-1}/0.2 C/100th cycle	S2
KOH activated graphene	2313	67	1007 mAh g^{-1}/0.2 C/60th cycle	S3
Graphene sheets reduced by Na_2S		75.2	662 mAh g^{-1}/0.6 C/100th cycle	S4
Raw graphene		44.5	819 mAh g^{-1}/0.05 C/100th cycle	S5
Ethanol derived porous graphene		22	600 mAh g^{-1}/0.03 C/40th cycle	S6
Reduced graphene oxide		63.6	803 mAh g^{-1}/0.186 C/80th cycle	S7
Graphene		87	500 mAh g^{-1}/0.2 C/50th cycle	S8
GO with epoxy and hydroxyl groups		66	954 mAh g^{-1}/0.1 C/50th cycle	S9
Graphene-CNT hybrid	806	60	530 mAh g^{-1}/1 C/100th cycle	S10
Graphene membrane		67	600 mAh g^{-1}/0.1 C/100th cycle	S11
Fibrous graphene		63	700 mAh g^{-1}/0.18 C/100th cycle	S12
Scotch-tape-like exfoliated graphene		73	835 mAh g^{-1}/0.5 C/10th cycle	S13
Reduced graphene oxide coating	598	63	803 mAh g^{-1}/0.12 C/160th cycle	S14
GlM	2700	43.6 62.8 72.3	1067 mAh g^{-1}/0.5 C/300th cycle 960 mAh g^{-1}/0.5 C/200th cycle 854 mAh g^{-1}/0.5 C/200th cycle	This work

PEG: poly(ethylene glycol), GO: graphene oxide.

References

S1 Y. Y. Li, Z. S. Li, P. K. Shen, *Adv. Mater.*, 2013, **25**, 2474-2480.

S2 H. Wang, Y. Yang, Y. Liang, J. T. Robinson, Y. Li, A. Jackson, Y. Cui, H. Dai, *Nano. Lett.*, 2011, **11**, 2644-2647.

S3 B. Ding, C. Z. Yuan, L. F. Shen, G. Y. Xu, P. Nie, Q. X. Lai, X. G. Zhang, *J. Mater. Chem. A*, 2013, **1**, 1096-1101.

S4 Z. K. Wei, J. J. Chen, L. L. Qin, A. W. Nemage, M. S. Zheng, Q. F. Dong, *J. Electrochem. Soc.*, 2012, **159**, A1236-A1239.

S5 B. Wang, K. Li, D. Su, H. Ahn, G. Wang, *Chem. -Asian J.*, 2012, **7**, 1637-1643.

S6 J. Z. Wang, L. Lu, M. Choucair, J. A. Stride, X. Xu, H. K. Liu, *J. Power Sources*, 2011, **196**, 7030-7034.

S7 H. Sun, G.-L. Xu, Y.-F. Xu, S.-G. Sun, X. Zhang, Y. Qiu, S. Yang, *Nano Res.*, 2012, **5**, 726-738.

S8 S. Evers, L. F. Nazar, *Chem. Commun.*, 2012, **48**, 1233-1235.

S9 L. Ji, M. Rao, H. Zheng, L. Zhang, Y. Li, W. Duan, J. Guo, E. J. Cairns, Y. Zhang, *J. Am. Chem. Soc.*, 2011, **133**, 18522-18525.

S10 M. Q. Zhao, X. F. Liu, Q. Zhang, G. L. Tian, J. Q. Huang, W. Zhu, F. Wei, *ACS. Nano*, 2012, **6**, 10759-10769.

S11 J. Jin, Z. Wen, G. Ma, Y. Lu, Y. Cui, M. Wu, X. Liang, X. Wu, *RSC Adv.*, 2013, **3**, 2558-2560.

S12 G. M. Zhou, L. C. Yin, D. W. Wang, L. Li, S. F. Pei, I. R. Gentle, F. Li, H. M. Cheng, *ACS. Nano.*, 2013, **7**, 5367-5375.

S13 T. Lin, Y. Tang, Y. Wang, H. Bi, Z. Liu, F. Huang, X. Xie, M. Jiang, *Energy Environ. Sci.*, 2013, **6**, 1283-1290.

S14 N. Li, M. Zheng, H. Lu, Z. Hu, C. Shen, X. Chang, G. Ji, J. Cao, Y. Shi, *Chem Commun*, 2012, **48**, 4106.